18th International Conference on Structural Mechanics in Reactor Technology (SMiRT 18)
Beijing, China, August 7-12, 2005
SMiRT18-G04-1

ON THE CONSTRAINT-BASED FAILURE ASSESSMENT OF THICK-WALLED CYLINDERS WITH INTERNAL AXIAL CRACKS

Xin Wang
Department of Mechanical and Aerospace Engineering, Carleton University, Ottawa, Ontario, Canada, K1S 5B6
E-mail: xwang@mae.carleton.ca

Wolf Reinhardt
Nuclear Engineering, Babcock & Wilcox Canada, Cambridge, Ontario, Canada, N1R 5V6
E-mail: wdreinhardt@babcock.com

ABSTRACT

The loss of crack tip constraint in a cracked structure leads to enhanced resistance to both cleavage and ductile tearing. However, conventional failure assessment schemes (CEGB-R6, BS-7910) use lower bound toughness obtained from highly constrained test specimens. Cracks in many real engineering structures are not highly constrained, which makes failure predictions using conventional failure assessment schemes based on lower bound fracture toughness values overly conservative. Excessive conservatism in the structural assessment can lead to unwarranted repair or decommissioning of structures, and thus cause unneeded cost and inconvenience. Recent developments on constraint-based fracture mechanics have enabled analysts to perform a practical assessment of defective components including constraint effects. For example, the recently developed structural integrity assessment procedures for European industry (SINTAP) have suggested a framework of failure assessments that includes the constraint effect. In this paper, the application of constraint-based failure assessment to axial cracks in thick-walled cylinders is presented. The cylindrical component considered is a nuclear reactor head nozzle. The *T*-stress is used as the constraint parameter. It is demonstrated that the predicted internal pressure level corresponding to failure increases as much as 40%-60% once the constraint effect has been considered in the assessment.

Keywords: Fracture, Failure Assessment, Thick-Walled Cylinders, Constraint Effect.

1. INTRODUCTION

Fracture assessments of cracked structures using the failure assessment diagram approach are well established [1, 2]. However, all these conventional failure assessment schemes use a lower bound fracture toughness obtained from highly constrained test specimens. Over-conservative assessments may sometimes occur in situations where the crack in a component is under conditions of low constraint. Constraint effects on fracture have, therefore, received considerable attention recently in efforts to reduce the conservatism of the analysis. Two parameter, (J, T) or (J, Q), fracture mechanics has been developed to describe the stress and strain fields ahead of a crack tip under various loading conditions corresponding to different constraint levels [3, 4]. Here J is the J-integral, while T is the elastic T-stress, and Q is the hydrostatic Q-stress which are the so-called constraint parameters. Based on two-parameter fracture mechanics, the framework for including constraint effect in the failure assessment diagram approach was proposed [5]. The recent version of R6 [1], and the newly developed structural integrity assessment procedures for European industry (SINTAP) [6], have suggested the procedures for failure assessment which includes the constraint effect.

A thick-walled pressure vessel with an internal edge crack (Figure 1) represents a typical geometry of a nozzle on the nuclear reactor head. An edge crack is postulated to exist in the nozzle wall, and the maximum allowable internal pressure decreases from the design pressure because of the existence of the edge crack. The assessment of such component is of great importance for the life estimation of these structures. It has been

observed [7] that an edge crack in a thick-walled cylinder under internal pressure load is under low constraint conditions. It is therefore advantageous to include the lower constraint effects when conducting the failure assessment. In doing so, excessive conservatism in the assessment can be removed and unwarranted repair or decommissioning of structures can be avoided.

In this paper, the constraint-based failure assessment of an edge cracked thick-walled cylinder under internal pressure load is presented. In section 2, the constraint-based failure assessment diagram approach is summarized. In section 3, the calculation of fracture parameters including stress intensity factors, *T*-stress and the limit loads for cylinders with an edge crack are presented. In section 4, the failure assessment is conducted. It is demonstrated that when the lower constraint effect is properly accounted for, the maximum allowable internal pressure level can increase significantly.

2. CONSTRAINT-BASED FAILURE ASSESSMENT DIAGRAMS

In this section, the constraint-based failure assessment diagram procedure is outlined. Allowance for constraint effects in the failure assessment diagram approach was first introduced into the R6 procedure [1] and recently included in SINTAP procedures [6]. A procedure that follows the R6 recommendations [1] is outlined here.

The conventional failure assessment diagram methods embedded in R6 [1] and BS7910 [2] are essentially single parameter procedures in that fracture is assumed to be governed by a single value of toughness or crack opening displacement. The assessment of the potential of failure is determined by the two dimensionless calculated parameters, (K_r, L_r), determined from

$$K_r = \frac{K_I}{K_{IC}} \tag{1}$$

and

$$L_r = \frac{\sigma}{\sigma_L} \tag{2}$$

Here K_r is the stress intensity ratio with K_I being the stress intensity factor for the cracked component and K_{IC} the toughness of the material. The parameter L_r is the stress ratio, which is the ratio of the applied stress to the limit stress solution of the cracked component calculated based on the yield stress. Failure is avoided if this point (K_r, L_r) lies within a failure assessment diagram, represented by a curve, $K_r = f(L_r)$ and at the same time L_r is less than a cut-off value $L_r^{\max}$.

Based on two parameter fracture mechanics, R6 [1] (Appendix 14) recognizes that a fracture resistance K_{mat}^{C} relevant to conditions of low constraint, may exceed the conventional fracture resistance K_{IC} measured under conditions of high constraint. To include this effect, it was suggested that the failure assessment diagram is modified to:

$$K_r = f(L_r)\left(\frac{K_{mat}^{C}}{K_{IC}}\right) \tag{3}$$

Following detailed theoretical and experimental analysis [3-5], this increase in fracture toughness can be represented by the following relationship:

$$K_{mat}^{C} = K_{IC}\left[1+\alpha(-\beta L_r)^m\right] \tag{4}$$

where α, and m are material dependent constants, which define the dependence of fracture toughness on constraint; and β is a normalized constraint parameter. Substituting (4) into (3), we have

$$K_r = f(L_r)\left[1+\alpha(-\beta L_r)^m\right] \tag{5}$$

Equation (5) is the constraint-based failure assessment diagram. Failure is avoided if assessment point (K_r, L_r) (calculated from Eqs. (1) and (2)) lies within Eq. (5) and L_r is less than a cut-off value $L_r^{\max}$.

The normalized constraint parameter β is defined from the hydrostatic *Q*-stress or the elastic *T*-stress:

$$\beta = \frac{Q}{L_r} = \frac{T}{\sigma_Y L_r} \tag{6}$$

where σ_Y is the yield stress of the material. Note that here the following estimation of *Q* stress in terms of *T*-stress is used [5]:

$$Q = \frac{T}{\sigma_Y} \tag{7}$$

To conduct constraint-based assessment for a cracked body, in addition to the knowledge of the stress intensity factor and the limit load for cracked components, the *T*-stress or the *Q* stress is required.

3. FRACTURE PARAMETERS SOLUTIONS FOR EDGE-CRACKED THICK-WALLED CYLINDERS

In this section, the calculation of fracture parameters: stress intensity factor, elastic *T*-stress and the limit load for edge-cracked thick-walled cylinders are presented. Figure 1 shows the geometry considered. Here R_i and R_o are the internal and external radius, t is the wall thickness, and a is the crack depth. The loading condition is internal pressure.

3.1 Stress Intensity Factor Solution

The stress intensity factor solutions for edge cracks in thick-wall cylinders were obtained using finite element methods by different authors [8, 9]. For internal pressure, p, the stress intensity factors were presented as follows:

$$K = Y \cdot p \cdot \sqrt{\pi a} \tag{8}$$

where the Y is the normalized stress intensity factor, the results for wide range of thick-walled cylinder geometries with edge cracks, $1.5 \le R_o/R_i \le 2.5$ and $0 \le a/t \le 0.6$, are presented in Tables in [9]. In the current analysis, stress intensity factors used are from Ref. [9]. The normalized numerical solutions together with the least square fitting of the data are plotted in Figure 2.

3.2 Elastic *T*-Stress Solution

Recently, *T*-stress solutions were developed using boundary element method for cracks in thick-walled cylinders [7, 10]. In [7, 10], *T*-stress solutions for geometries of $1.5 \le R_o/R_i \le 2.5$ and $0 \le a/t \le 0.6$ are presented for a wide range of loading conditions. For internal pressure loading, the *T*-stress is given as:

$$K = V \cdot p \tag{9}$$

The V is the normalized *T*-stress, which are presented in tables in Ref. [10]. The normalized *T*-stresses solutions are plotted in Figure 3 for different R_o/R_i ratios. Least square fittings of the data are plotted. It can be seen that edge-cracked thick-walled cylinders are under low constraint conditions (i.e. the *T*-stress is negative).

3.3 Limit Load Solution

Different limit load solutions for cracked thick-walled cylinders under internal pressure are presented by various authors [11]. In the current work, the expression proposed in [12] for edge cracks is used:

$$p_0 = \frac{2(t-a)\sigma_Y}{\sqrt{3}(R_i + a)} \tag{10}$$

4. FAILURE ASSESSMENTS

Based on the stress intensity factor, *T*-stress and limit load solutions presented in the last section, the failure assessments of edge cracked thick-walled cylinders are conducted. The load condition considered is internal pressure. The cylinder geometry considered is for a reactor head nozzle, with R_o/R_i = 2.5, and R_o = 48 mm. Cracks of relative crack depth, a/t = 0, 0.1, 0.2…0.6, are considered. The material used is alloy 600. At operating temperature, the following material properties are used: tensile yield stress = 310 MPa and ultimate strength = 786 MPa. The Young's modulus of the material is 207GPa. The fracture toughness of the material K_{IC} is assumed to be 200 MPa$\sqrt{m}$ based on a conservative estimation. Constraint related material constants α, and m, which define the dependence of fracture toughness on constraint, are assumed to be 1.5 and 1 [5], respectively. For each crack geometry, the maximum allowable internal pressure p_{max} that can be applied without failure is obtained from the failure assessment diagram. The cracked cylinder is initially assessed using the conventional FAD procedure, and then reassessed using the constraint-based procedure.

In the present analysis, the failure assessment diagram approach of Level 3 of PD7910 [2] is used. In [2], a lower bound FAD curve that is independent of geometry and the material stress-strain curve is given by:

$$K_r = (1 - 0.14 L_r^2)\left[0.3 + 0.7\exp(-0.65 L_r^6)\right] \tag{11}$$

Since the load ratio is defined in terms of the yield strength, L_r can be great than 1. The typical cut-off is 1.2 for C-Mn Steel and 1.8 for austentic stainless steel [2]. In the current analysis, since the flow stress σ_f is known for the material used, which is equal to $0.5(\sigma_y + \sigma_u)$, the ratio of flow stress to the yield stress, σ_f/σ_y = 1.767, is used as the cut-off. Figure 4 shows a plot of the failure assessment diagram.

The resulting maximum allowable internal pressure is normalized as follows:

$$P_n = \frac{p_{\max}}{\sigma_f} \tag{12}$$

where σ_f is the flow stress of the material equals $0.5(\sigma_y + \sigma_u)$, with σ_y and σ_u yield and ultimate strengths, respectively. The resulting maximum normalized internal pressures P_n for different *a/t* ratios are presented in Figure 5.

Then the constraint-based assessment is conducted. From Eq. (5), the constraint-based failure assessment curve is given by:

$$K_r = (1 - 0.14L_r^2)\left[0.3 + 0.7\exp(-0.65L_r^6)\right]\left[1 + 1.5(-\beta L_r)\right] \quad (13)$$

The resulting FAD curves for the current analysis are plotted in Figure 4. Based on Eq. (13), the maximum normalized internal pressure P_n for different *a/t* ratios are obtained and presented in Figure 5. It can be observed that it is overly conservative to exclude the low constraint effect. By accounting for the effect of low constraint, the increase in the allowable internal pressure can be as much as 60% for shallow cracks (*a/t* = 0.1-0.2) and about 40% for deep cracks (*a/t* = 0.6).

5. CONCLUSIONS

In this paper, the constraint-based failure assessments of edge cracked thick walled cylinder under internal pressure load are presented. The constraint-based failure assessment diagram approach is described. The calculation of fracture parameters including stress intensity factors, *T*-stress and the limit loads for edge-cracked thick wall cylinders were presented. The failure assessments are conducted for typical reactor head nozzle geometry with various crack depth. It is demonstrated that when the lower constraint effect is properly accounted for, the maximum allowable internal pressure can increase by as much as 40%-60%.

REFERENCES

1. R6, 1997, "Assessment of the Integrity of Structures Containing Defects, Procedure R6, Revision 3," Nuclear Electric Ltd. Gloucester, U.K.
2. BS 7910:1991, August 1991, "Guidance on Some Methods for the Derivation of Acceptance Levels for Defects in Fusion Welded Joints", British Standards Institution.
3. O'Dowd, N.P. and Shih, C.F., 1991, "Family of Crack Tip Fields Characterized by a Triaxiality Parameter," *Journal of Mechanics and Physics of Solids*, Vol. 39, pp. 989-1015.
4. Betegon, C., Hancock, J.W., 1991, "Two-Parameter Characterization of Elastic-Plastic Crack Tip Fields," *ASME Journal of Applied Mechanics*, Vol. 58, pp. 104-110.
5. Ainsworth, R.A. and O'Dowd, N.P., 1995, "Constraint in the Failure Assessment Diagram Approach for Fracture Assessment," *ASME Journal of Pressure Vessel Technology*, Vol. 117, pp. 260-267.
6. Ainsworth, R.A., Sattaru-Far, I., Sherry, A.H., Hooton, D.G. and Hadley, I., 2000, "Methods for Including Constraint Effects within the SITAP Procedures," *Engineering Fracture Mechanics*, Vol. 67, pp. 563-571.
7. Li, J., C.L. Tan and X. Wang, 2004, "Weight Functions for *T*-stress for Edge Cracks in Thick-Walled Cylinders," *Proceedings of ASME Pressure Vessel and Piping Conference*, PVP- Vol. 482, pp. 99-104.
8. Andrasic, C. P. and Parker, A.P., 1984, "Dimensionaless Stress Intensity Factors for Cracked Cylinders under Polynomial Crack Face Loadings", *Engineering Fracture Mechanics*, Vol. 19, pp. 187-193.
9. Wu, X.R. and Carlsson, A.J., 1991, "Weight Functions and Stress Intensity Factors", Pergamon Press.
10. Li, J. 2003, "The Evaluation of *T*-stress Using Boundary Element Method", Master's Thesis, Dept. of Mechanical and Aerospace Engineering, Carleton University, Ottawa, Canada.
11. Miller, A.G., 1988, "Review of Limit Loads of Structures Containing Defects", *International Journal of Pressure Vessels and Piping*, Vol. 32, pp. 197-327.
12. Kumar, V., German, M.D. and Shih, C.F., 1981, " An Engineering Approach for Elastic-Plastic Fracture Analysis", *EPRI Report* NP-1931, Electric Power Research Institute, Palo Alto, CA, USA.

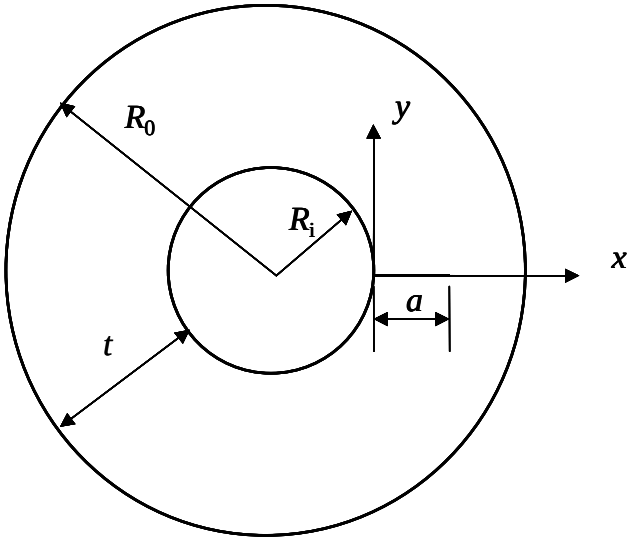

Figure 1 An edge crack in a thick walled cylinder

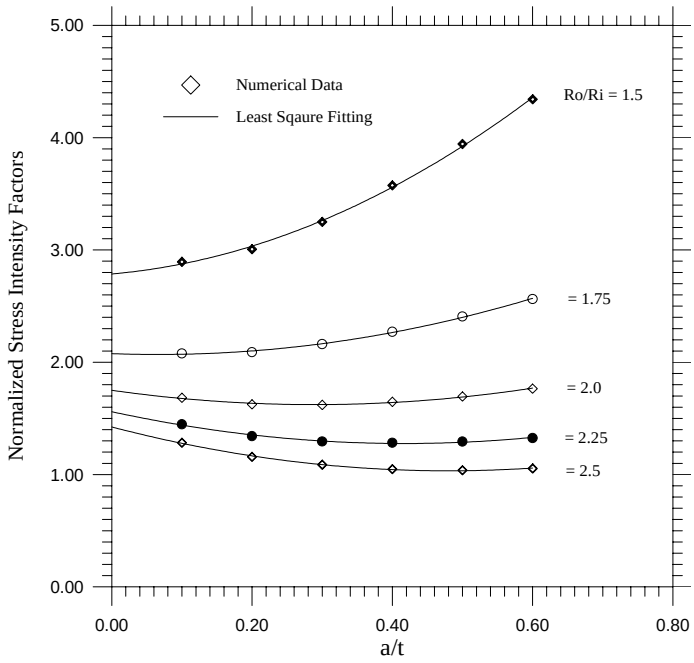

Figure 2 Stress intensity factors for edge cracks in thick-walled cylinders

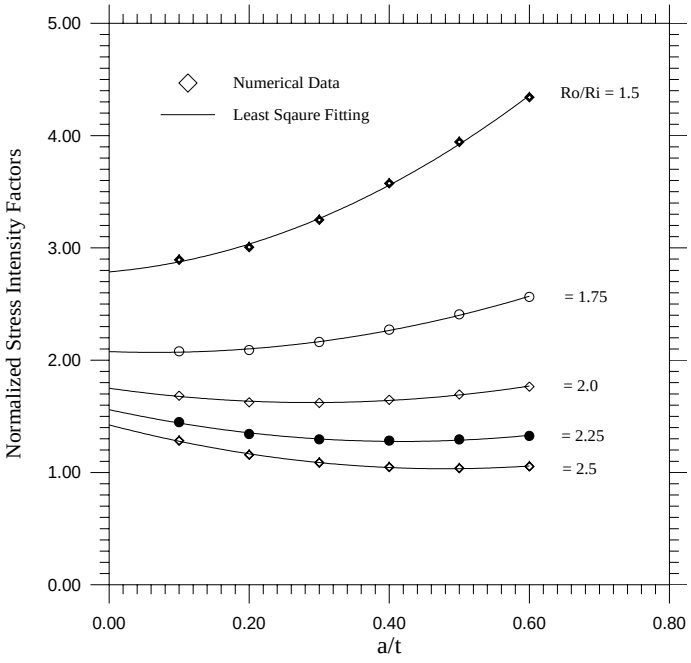

Figure 3 T-stress for edge cracks in thick-walled cylinders

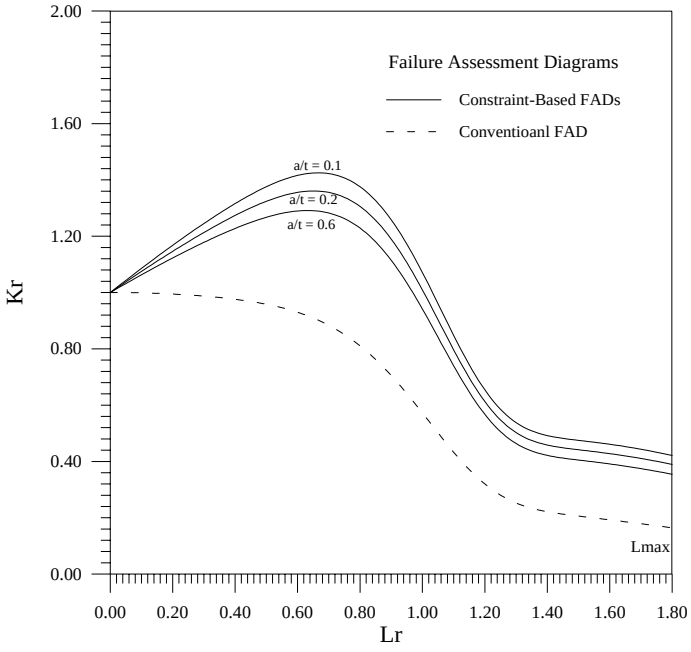

Figure 4 Failure assessment diagrams

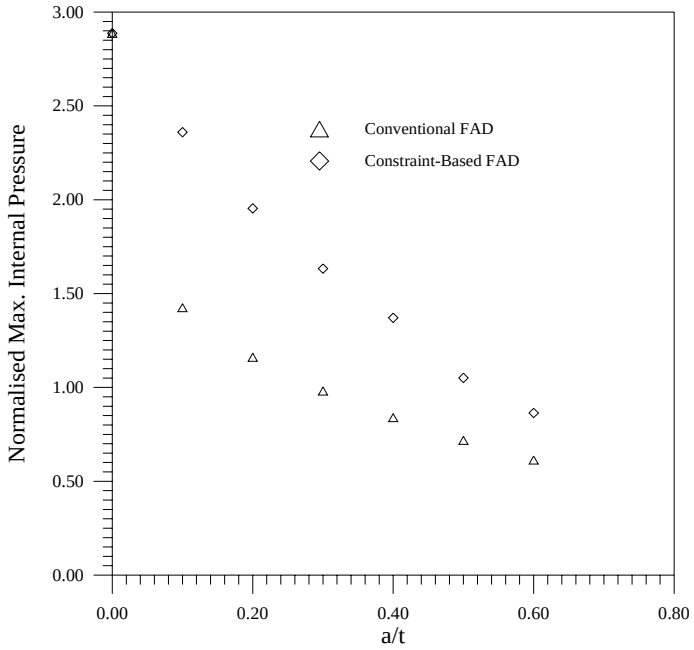

Figure 5 Maximum internal pressure results from assessment